Modal parameter estimation of a lightly damped symmetric plate using Direct Estimation of Residues from Rational-fraction Polynomials

Nimish Pandiya, Wim Desmet

MODAL PARAMETER ESTIMATION OF A LIGHTLY DAMPED SYMMETRIC PLATE USING DIRECT ESTIMATION OF RESIDUES FROM RATIONAL-FRACTION POLYNOMIALS

Nimish Pandiya[1,2] **Wim Desmet**[2,3]
[1] Center of Competence for Vibration, Robert Bosch GmbH,
Postfach 30 02 40, 70442 Stuttgart, Germany
[2] Department of Mechanical Engineering, KU Leuven,
Celestijnenlaan 300-B, 3001 Leuven, Belgium
[3] DMMS Lab, Flanders Make, Leuven, Belgium
nimish.pandiya@de.bosch.com

ABSTRACT

The newly introduced algorithm named Direct Estimation of Residues from Rational-fraction Polynomials (DERRP), is useful for computing a dynamic system's modal parameters in a single step. This algorithm is applied in the frequency domain and leverages the computation of numerator coefficients to compute partial fraction residues using a recursive computation. In the presented work, key features of the algorithm are emphasized under the well-established Unified Matrix Polynomial Approach framework. The algorithm is applied to an experimental frequency response function data-set obtained from a lightly-damped metallic plate and the results are discussed. It is concluded that the estimates of all the modal parameters, namely, natural frequencies, mode shapes, modal participation factors and modal scaling factors, are well characterised even in the presence of (pseudo-) repeated roots. The positive results build a high confidence for further use of the DERRP algorithm for experimental modal analysis.

1. INTRODUCTION

Modal parameter estimation (MPE) refers to system identification of vibrating structures from experimental or digitally acquired data. The parameters that define the dynamic behavior of a mechanical structure are defined in the "modal" domain and are namely the resonance frequencies, damping ratios, mode shapes and (for multi-reference cases) participation vectors [1, 2]. Current state of the art algorithms utilize (experimental) frequency response function data-sets to fit an *a-priori* mathematical model that is nonlinear in the said parameters 1. This process is carried out in two distinct steps. First, a rational-fraction polynomial is fit to the data in a least-squares sense. The poles are estimated via an eigen-value decomposition of a companion matrix constructed using the estimated denominator polynomial coefficients. The eigen-vectors thus obtained represent the participation vectors, while the complex eigen-values include the damping ratio and the resonance frequency information. This process is carried out for increasing model orders of the rational fraction model. Once the resonances and associated vectors are obtained, valid structural poles must be filtered out from a larger set of computed poles, typically from a stabilization or consistency diagram. Using these selected eigen-values and vectors, in the second step, the remaining set of vectors i.e. the mode shape vectors, the modal scaling factor and the out-of-band residuals are estimated by fitting the subset of poles selected and the initial data-set [3,4]. As highlighted by Allemang *et al.* in [5], the dimensions may be decided by formulating the using a left or right matrix description, depending on which eigen-vectors obtained in the first step may alternately represent modal vectors. Subsequently, in the second-step post the user's selection of valid poles, participation vectors may be computed.

The recently introduced algorithm labeled as Direct Estimation of Residues from Rational-fraction Polynomials [6] is shown to utilize the previously discarded or unused numerator polynomial coefficients to compute the complete set of modal parameters in a single computation step. The advantage lies in the fact that the second-stage computation of a subset of modal parameters (namely, the scaled modal vectors) is eliminated and the consistency or the stabilization chart can be plotted with complete modal information. This increases the confidence of the user in the pole selection phase, which is essentially transformed to the model validation step if multiple frequency bands of interest are not merged. In this paper, the algorithm is applied to FRFs obtained from a square plate, where, due to symmetry in the geometry of the structure, pseudo-repeated modes are expected to be observed.

2. THE DERRP ALGORITHM: AN OVERVIEW

This section provides a brief overview of the steps involved in the DERRP algorithm for computation of modal parameters from experimentally (or simulated) frequency response function (FRF) data. For a more detailed description of the algorithm, the reader is directed to [7, 8]. Since the paper discusses an impact testing campaign, the number of inputs represents the long dimension of the data-set and the the number of outputs represents the short dimen-

sion per frequency. However, it must be noted that a similar appraoch is possible for both the right-matrix description and for the case of transposed FRFs in the left-matrix description as shown. Additionally, the formulations discussed are valid for displacement-force type FRFs (compliance FRFs) for linear, time-invariant systems.

The modal representation of FRFs in a partial fraction form is shown in Eqn. (1). The equation highlights the relation of the modal parameters with the FRF matrix and also includes the effect of out-band-modes in the form of lower and upper residuals.

$$\begin{aligned}\Big[H(\omega)\Big]_{N_o \times N_i} = \\ \sum_{r=1}^{N_r} \left(\frac{[A_r]_{N_o \times N_i}}{j\omega - \lambda_r} \frac{[A_r]^*_{N_o \times N_i}}{j\omega - \lambda_r^*} \right) \\ + \frac{[LR]_{N_o \times N_i}}{(j\omega)^2} + [UR]_{N_o \times N_i}\end{aligned} \tag{1}$$

Here, $[H(\omega)] \in \mathbb{C}^{N_o \times N_i}$ is the complex multiple-input multiple-output transfer function in the Fourier ($j\omega$) domain, N_o is the number of outputs, N_i is the number of inputs and N_r is the number of conjugate mode pairs ($\lambda_r, \lambda_r^* = \sigma \pm j\Omega$). $[A_r] \in \mathbb{C}^{N_o \times N_i}$ represent the residue at the modal frequency λ_r. The lower and upper residuals $[LR] \in \mathbb{C}^{N_o \times N_i}$ and $[UR] \in \mathbb{C}^{N_o \times N_i}$ represent the out-of-band influence in the frequency range of interest.

The residue at the r^{th} modal frequency *i.e.* $[A_r]$ may be decomposed into the modal scaling factor $Q_r \in \mathbb{C}^{1\times 1}$, modal vector $\psi_r \in \mathbb{C}^{N_o \times 1}$ and modal participation vector $L_r \in \mathbb{C}^{N_i \times 1}$ as shown in Eqn. (2). The residue is of unity rank, which is an important property for experimentally obtained FRFs, since, in reality, truly repeated modes do not occur. It is to be noted that from hereon, the modal scaling factor may be omitted by incorporating it in the mode shape vector, making it the *scaled* mode shape vector.

$$\big[A_r\big]_{N_o \times N_i} = Q_r \big\{\psi_r\big\}_{N_o \times 1} \big\{L_r\big\}^T_{1 \times N_i} \tag{2}$$

The DERRP model identifies that the expansion of the partial fraction model shown in Eqn. (1) leads to a rational fraction description of the form shown in Eqn. (3). This formulation is in a left-matrix descriptor form, but the algorithm also holds true for the right-matrix description as well.

$$\left[\sum_{i=0}^{m} \Big[[\alpha_i][H(s)]s^i\Big]\right] = \left[\sum_{i=-2}^{m} \Big[[\beta_i][I]s^i\Big]\right] \tag{3}$$

Here, $[H(s)] \in \mathbb{C}^{N_o \times N_i}$ represents the transfer function in the complex Laplace domain and the order of the "numerator" ($[\beta_i] \in \mathbb{C}^{N_o \times N_i}$) and "denominator" ($[\alpha_i] \in \mathbb{C}^{N_o \times N_o}$) matrix coefficient polynomials is indicated by m. The inclusion of residuals is ensured by defining the numerator polynomial from a degree of -2.

An over-determined system of equations in the unknowns $[\alpha_i]$ and $[\beta_i]$ may be defined by using Eqn. (3) for each independent frequency line. This system is solved in a least-squares sense after normalizing the lowest model order denominator matrix coefficient $[\alpha_0]$ to an identity matrix to limit the null-space solution.

Post the computation of the matrix-coefficients of the left-matrix rational fraction description, a recursive algorithm introduced by Vu is carried out on the denominator polynomial [9]. The result is that the inverse of the square denominator polynomial matrix may be represented in terms of an adjoint matrix-coefficient ($[\alpha_i^A]$) polynomial and a monic (d_i) characteristic equation. This allows the transfer function to be represented in the form shown in Eqn. (4) in the Laplace domain.

$$\begin{aligned}&\Big[H(s)\Big]_{N_o \times N_i} \\ &= \sum_{r=1}^{N_r} \left(\frac{[A_r]_{N_o \times N_i}}{s - \lambda_r} + \frac{[A_r]^*_{N_o \times N_i}}{s - \lambda_r^*} \right) + \\ &\quad \frac{[LR]_{N_o \times N_i}}{s^2} + [UR]_{N_o \times N_i} \\ &= \frac{\left[\sum\limits_{i=0}^{(N_o-1)m} \Big[[\alpha_i^+]s^i\Big]_{N_o \times N_o}\right]\left[\sum\limits_{i=-2}^{m} \Big[[\beta_i]s^i\Big]_{N_o \times N_i}\right]}{\sum\limits_{i=0}^{N_o m} d_i s^i}\end{aligned} \tag{4}$$

Complex natural frequencies ($\lambda = \sigma + j\omega$) are computed as the roots of the characteristic equation [10]. The imaginary part (ω) represents the natural frequency and the damping ratio (ζ) may be computed using the real part (σ) as shown in Eqn. (5).

$$\zeta = \frac{\sigma}{|\lambda|} \tag{5}$$

Scaled residues ($[A]_{N_o \times N_i}$) are computed for each complex natural frequency (or pole) by evaluating the limit $\lim_{s\to\lambda}[H(s)](s-\lambda)$ using Eqn. (4). The fractional limit is of an indeterminate form as both the numerator (due to the $(s-\lambda)$ factor) and the denominator (due to λ being the root of the characteristic equation) are undefined at λ. The explicit evaluation of the limit for an r^{th} pole is shown in Eqn. (6) by applying the well known L-Hospital's rule.

$$\Big[A_r\Big]_{N_o \times N_i} = \frac{\left[\sum\limits_{i=0}^{(N_o-1)m} \Big[[\alpha_i^+]\lambda_r^i\Big]\right]\left[\sum\limits_{i=-2}^{m} \Big[[\beta_i]\lambda_r^i\Big]\right]}{\sum\limits_{i=1}^{N_o m} i d_i \lambda_r^{i-1}} \tag{6}$$

The residues for each poles may be summed along the appropriate dimension to result in the participation ($\{L_r\}_{N_i \times 1}$) and modal ($\{\psi_r\}_{N_o \times 1}$) vector estimates for the respective poles. In the cases where a particular form of modal scaling is required, the residue may be decomposed using singular value decomposition and the singular value may be scaled appropriately [2].

The out-of-band residuals can be computed as residues with pole values $s = 0$ (for $[LR]$) and $s = \infty$ (for $[UR]$).

Hence, at the end of this computational step, the complete set of modal parameters, and the lower and upper residuals are available to be selected via the stabilization diagram. The presence of the complete modal model model as described in Eqn. (1) allows the user to interactively select valid modes based on the error between measured and reconstructed FRFs. Additionally, complete model information in the stabilization diagram is also projected to allow for more robust automated pole selections using the existing state of the art processes [11, 12].

3. EXPERIMENTAL AND ALGORITHMIC SETUP

An experimental campaign was carried out on a $22cm \times 22cm \times 2.1cm$ square metallic plate. As shown in Fig. 1, a 8×8 grid was marked out on the plate to identify excitation points for an impact hammer. The plate was supported on depressurized tennis balls to create a free-free boundary condition environment and three accelerometers were placed on the bottom side of the plate, as shown in Fig. 2. The placement of the sensors in this manner allowed for eliminating impact location errors for obtaining driving point FRFs for the points marked in red (Fig. 1).

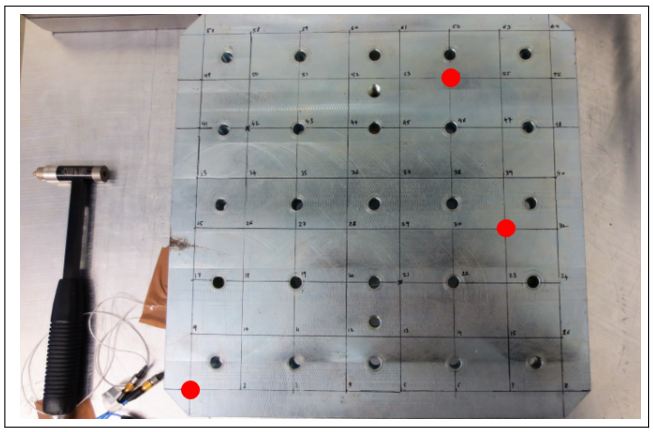

Figure 1. The aluminum alloy square plate used for the impact test campaign showing the grid used to locate impact locations and the response sensor locations, marked in red.

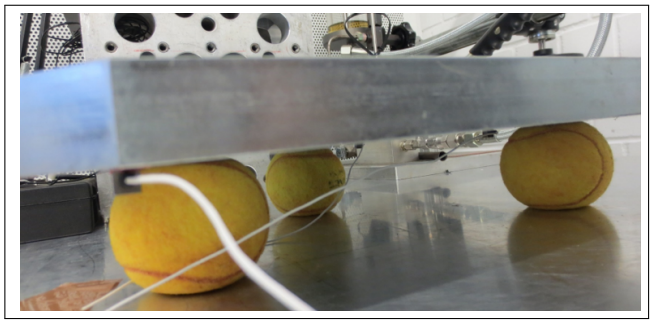

Figure 2. The structure in "free-free" boundary condition along with the sensors placed on the bottom-facing side of the plate.

Tab. 1 lists the setup parameters used for the impact testing of the structure. The acquired FRF matrix was of the size $[3 \times 64 \times 8192]$ and was exported from Siemens TestLab® in the universal file format to be read in MatLab®.

Spectral Lines	8192
Acquisition Time	2 seconds
FRF Estimator	H_1
Window	Uniform (Rectangular)
Averages	5

Table 1. Data acquisition setup for impact hammer testing on the square plate using SCADAS front-end and Siemens TestLab®.

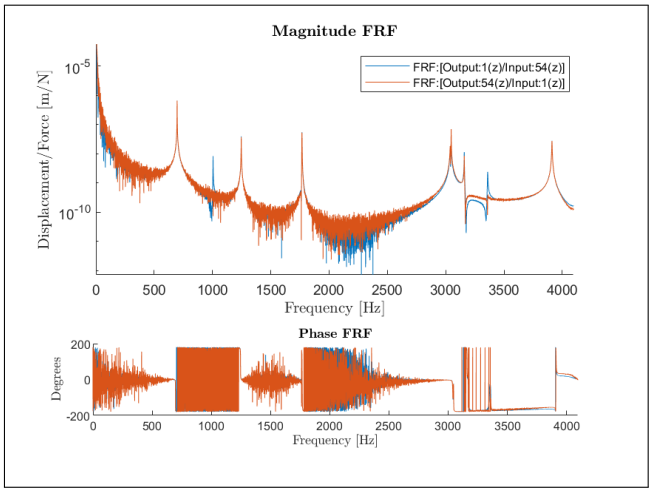

Figure 3. Reciprocity check for measurement degrees of freedom 1 and 54.

For model order determination, the Complex Mode Indicator Function (CMIF) [13] of the FRF set was used (Fig. 4). The maximum number of closely spaced (pseudo-repeated) modes was identified as 2 and for the construction of the stabilization diagram, a maximum denominator model order (m in Eqn. (3)) of 20 was selected.

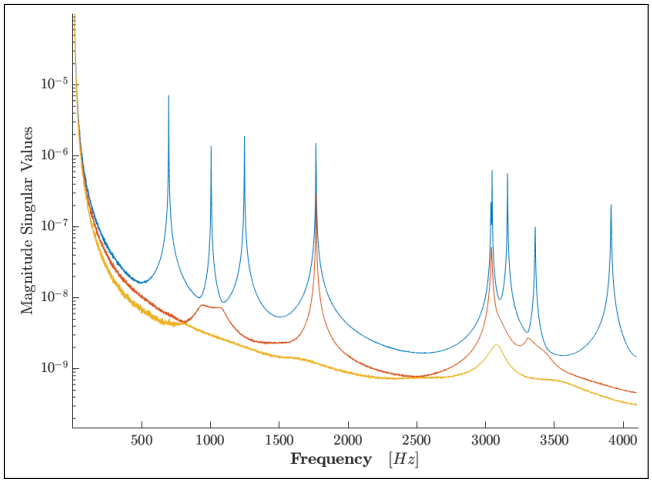

Figure 4. Complex mode indicator function (CMIF) of the FRF data-set for estimation of the model order.

The DERRP algorithm was deployed on the data-set in two bands as indicated in Tab. 2. The definition of the frequency bounds of these bands was arbitrary. The stabilization charts obtained for these bands can be seen in Fig. 5 and Fig. 6. The solid points indicate the selected poles. The consistency checks for the stabilization charts were carried out using tolerances shown in Tab. 3.

Band ID	1	2
Frequency from	414 Hz	2500 Hz
Frequency to	2500 Hz	4067 Hz
Expected number of modes	5	5

Table 2. Band definition for computation of modal parameters.

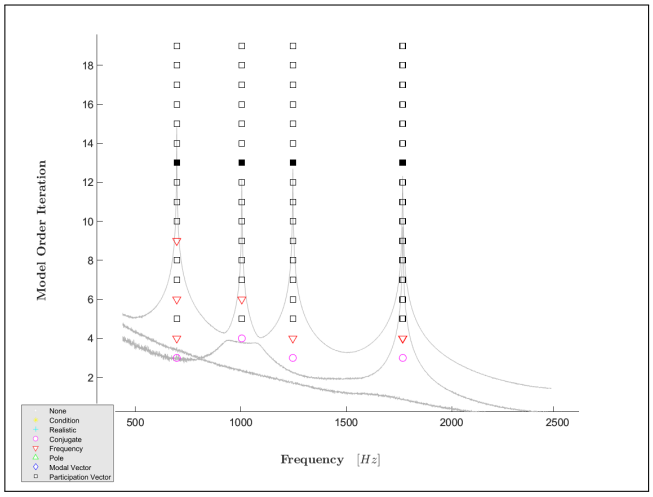

Figure 5. The modified stabilization chart for Band 1, showing poles with consistencies in modal and participation vectors only.

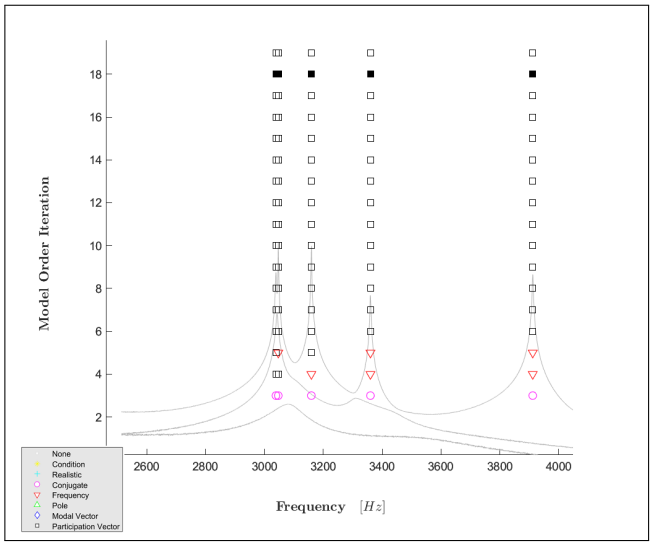

Figure 6. The modified stabilization chart for Band 2, showing poles with consistencies in modal and participation vectors only.

Conjugate (Hidden)	1%
Frequency (Hidden)	1%
Damping (Hidden)	5%
Modal Vector (Hidden)	2%
Participation Vector	2%

Table 3. Stabilization chart tolerances for the DERRP algorithm.

The vector consistencies are computed using the MAC formulation [14], while for values of frequencies and damping (including, conjugate check), a percentage difference formulation is utilized.

4. ESTIMATES OF MODAL PARAMETERS USING DERRP

The stabilization charts obtained for "Band 1" and "Band 2" are shown in Fig. 5 and Fig. 6 respectively. The black squares represent the poles with acceptable consistency in terms of the complete residue *i.e.* both modal and participation vectors. The selection of the poles was carried out manually in this case, however a cluster-based automated approach to poles selection is also possible while minimizing the error between the measured and the reconstructed FRFs (including residuals) in the frequency band of interest.

The poles selected using the two bands are listed in Tab. 4, according to their estimated frequencies, damping ratios and modal vector mean phase correlation (MPC) [2]. For a proportionally damped system, the modal residue is expected to be purely imaginary (mean phase of $\pm 90°$) and the scaling may performed such that the participation vectors are purely real. As an example, for Mode 1 in Tab. 4, the modal and participation vectors are plotted in Fig. 8.

Mode	**Frequency** [Hz]	**Damping Ratio** (ζ %)	**Mean Phase** (^{o})
1	696.76	0.0293	87.388
2	1004.94	0.0445	88.345
3	1246.69	0.0376	87.334
4	1766.46	0.0329	87.351
5	1768.03	0.0426	87.346
6	3038.90	0.0500	88.433
7	3046.95	0.0192	89.252
8	3159.31	0.0215	-89.453
9	3360.03	0.0427	-86.424
10	3911.73	0.0359	-69.262

Table 4. Modal parameters of the poles selected in the modified stabilization diagram.

The modal vectors thus obtained are also linearly independent and this can be shown using the Modal Assurance Criterion (MAC) plots in Fig. 7. The mode shapes are displacement mode shapes, and may be converted to acceleration mode shapes by using the respective squared-cyclic frequency factors.

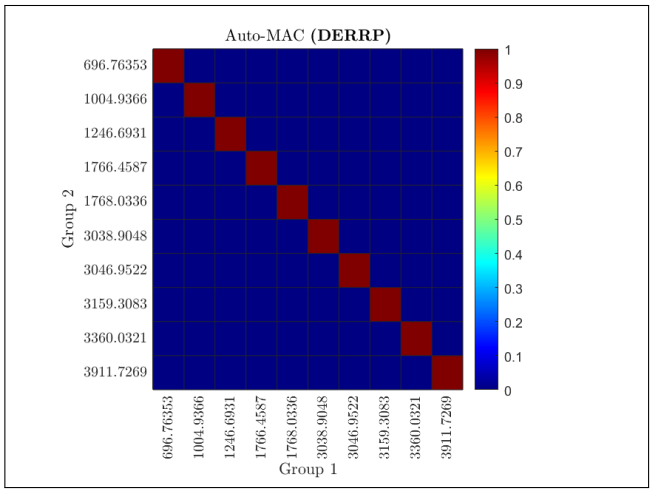

Figure 7. The auto-MAC plot for the modal vectors ($\{\psi\}_{64\times1}$).

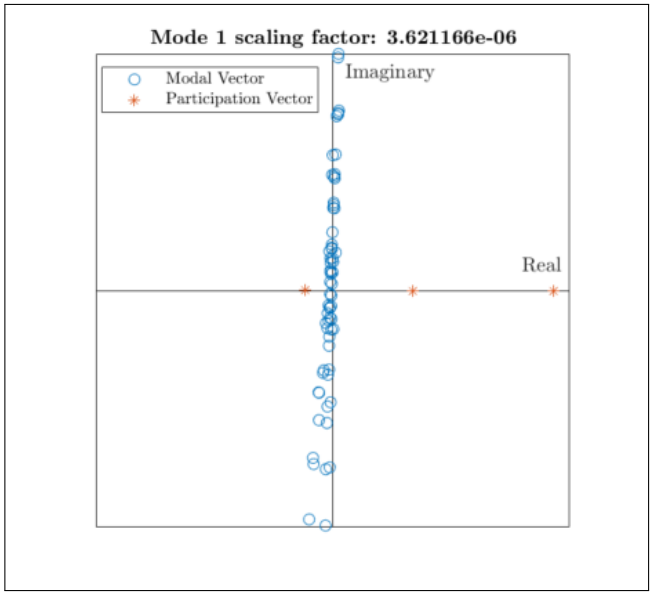

Figure 8. A plot of the modal and participation vectors obtained for Mode 1 in the complex plane.

5. MODEL VALIDATION

Once the quality of the modal parameters was determined to be satisfactorily good, FRF reconstruction was used as the means for model validation.The merging of the two bands involved re-computation of the residuals using the traditional partial fraction model. The FRFs obtained from the modal model can be seen plotted against the measured FRFs in Fig. 9 and Fig. 10. The two figures illustrate that the reconstruction of both the driving point and non-driving point FRFs are of good quality. The driving point FRF reconstruction is especially important since the numerator (Eqn. (4)) must include all the zeros [10] of the system at the particular degree of freedom. It is concluded from the quality of the reconstructed FRFs that the DERRP algorithm clearly facilitates high quality modal parameter estimates for experimental structures.

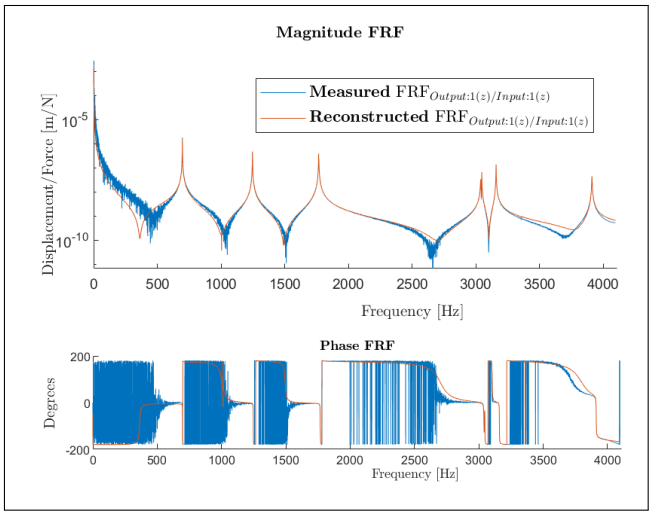

Figure 9. Comparison of the measured and reconstructed driving point FRFs at location 1.

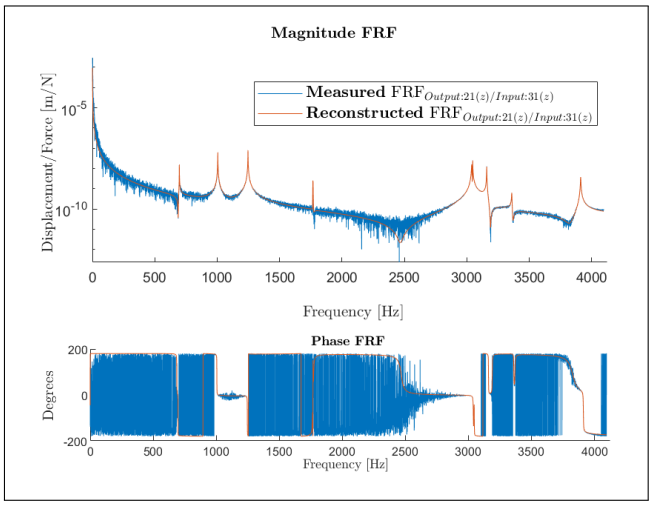

Figure 10. Comparison of the measured and reconstructed FRFs at input location 31 and output location 21.

6. CONCLUSIONS

In the presented work, the recently introduced DERRP algorithm was applied to a compliance FRF data-set (computed from an accelerance data-set) to obtain its modal parameters in the complete bandwidth. The analysis was carried out in two bands, and in each band, a well-defined estimate of the modes included was evident. Even though explicit out-of-band representations were estimated in the form of lower and Upper residuals for each band, they were recomputed due to combination of the bands. The key contribution here is the validation of the algorithm on an experimental data-set with (pseudo) repeated roots. The results shown are highly encouraging, and model validation indicated that an accurate modal model was identified using the method. The advantage of the method lies in the fact that all modal information is made available while plotting the "complete" stabilization (or consistency) diagram. The use of residue information in the diagram not

only provides a greater degree of statistical confidence in the pole-selection process, but is also expected to allow for complete and effective automation of the modal parameter estimation process.

7. ACKNOWLEDGMENTS

The authors gratefully acknowledge the European Commission for its support of the Marie Sklodowska Curie program through the ETN PBNv2 project (GA 721615).

8. REFERENCES

[1] J. M. M. e Silva and N. M. Maia, *Modal analysis and testing*. Springer Science & Business Media, 2012.

[2] W. Heylen, S. Lammens, and P. Sas, *Modal analysis theory and testing*. Faculty of Engineering. Department of Mechanical Engineering. Division of Production Engineering, Machine Design and Automation: KU Leuven, 1997.

[3] R. J. Allemang and D. Brown, "A unified matrix polynomial approach to modal identification," *Journal of Sound and Vibration*, vol. 211, no. 3, pp. 301–322, 1998.

[4] B. Peeters, H. Van der Auweraer, P. Guillaume, and J. Leuridan, "The polymax frequency-domain method: a new standard for modal parameter estimation?," *Shock and Vibration*, vol. 11, no. 3, 4, pp. 395–409, 2004.

[5] R. J. Allemang and D. L. Brown, "Experimental modal analysis and dynamic component synthesis. volume 1. summary of technical work," tech. rep., Structural Dynamics Research Lab, University of Cincinnati, OH, 1987.

[6] N. Pandiya, C. Dindorf, and W. Desmet, "A single step modal parameter estimation algorithm - computing residues from numerator matrix coefficients of rational fractions," in *Proceedings of the 38th International Modal Analysis Conference, A Conference and Exposition on Structural Dynamics, Houston*, Springer International Publishing, 2020.

[7] N. Pandiya and W. Desmet, "Direct estimation of residues from rational-fraction polynomials as a single-step modal identification approach," *Measurements and Signal Processing*, 2020. Submitted.

[8] N. Pandiya, "Direct estimation of residues from rational-fraction polynomials as applied to modal parameter estimation," Patent Application, EP 20154388.1, January, 2020.

[9] K. M. Vu, "An extension of the Faddeev's algorithms," in *2008 IEEE International Conference on Control Applications*, 9 2008.

[10] T. Kailath, *Linear systems*, vol. 156. Prentice-Hall Englewood Cliffs, NJ, 1980.

[11] A. W. Phillips, R. J. Allemang, and D. L. Brown, "Autonomous modal parameter estimation: methodology," in *Modal Analysis Topics, Volume 3*, pp. 363–384, Springer, 2011.

[12] P. Guillaume, P. Verboven, S. Vanlanduit, H. Van Der Auweraer, and B. Peeters, "A poly-reference implementation of the least-squares complex frequency-domain estimator," in *Proceedings of IMAC*, vol. 21, pp. 183–192, A Conference & Exposition on Structural Dynamics, Society for Experimental . . . , 2003.

[13] C. Shih, Y. Tsuei, R. Allemang, and D. Brown, "Complex mode indication function and its applications to spatial domain parameter estimation," *Mechanical systems and signal processing*, vol. 2, no. 4, pp. 367–377, 1988.

[14] R. J. Allemang, "The modal assurance criterion–twenty years of use and abuse," *Sound and vibration*, vol. 37, no. 8, pp. 14–23, 2003.